Stopping Cross Sections of Gases for α Particles from 0.3 to 2 MeV*

P. D. Bourland, W. K. Chu, and D. Powers
Baylor University, Waco, Texas 76703
(Received 22 July 1970)

Stopping cross sections for α particles have been measured in a differentially pumped gas-cell system from 300 keV to 2 MeV in 13 gaseous compounds: H_2, N_2, O_2, NH_3, N_2O, CO, CO_2, CH_4, C_2H_2, C_2H_4, C_2H_6, C_3H_6, and $(CH_2)_3$. The probable random error of the measurements varies from 1 to 2%. Independent measurements have also been made with a sealed gas cell in a scattering chamber for N_2 and H_2, and are found to agree with the differentially pumped gas-cell measurements to within 2.7%. Tests for water-vapor adsorption on thin carbon films used by Chu and Powers are also made and show that a deviation no greater than 3.8% would occur in their original dE/dx measurements.

I. INTRODUCTION

Renewed interest in the energy loss of α particles in gases has occurred in recent years. Park[1] measured dE/dx for 40- to 200-keV α particles in hydrocarbon gases. Palmer[2] obtained dE/dx for 1- to 8-MeV α particles in hydrocarbon gases at 500-keV intervals, and Rotondi,[3] for 0.1- to 5.3-MeV α particles in N_2, O_2, CH_4, and CO_2 by differentiating range-energy curves for these gases; these dE/dx measurements have quoted accuracies of 5% at 1 MeV and 8% at 500 keV or below. Rotondi[4] also measured dE/dx for 5-MeV α particles in N_2, O_2, CO, CO_2, NH_3, and hydrocarbon gases.

Deviation from the Bragg rule[5] for calculating molecular stopping cross sections from atomic stopping cross sections was found by two groups[6,7] for protons below 150 keV. Thus, deviation from Bragg's rule might then be expected for α particles below 600 keV.

Since there are only a very limited number of measurements of α-particle dE/dx in gaseous compounds in the energy region of possible Bragg-rule deviation, the purpose of the present experiment is to obtain a more detailed set of measurements and to test the applicability of Bragg's rule to the data so obtained. The present paper gives the results of the measurements, and the analysis of these measurements based on a study of the chemical binding is given in a separate paper.[8]

II. EXPERIMENTAL PROCEDURE

The Baylor 2-MeV Van de Graaff accelerator provides a singly charged helium-ion beam of energy 0.3–2 MeV. Two electrostatic beam steerers provide automatic ion-beam positioning along a prescribed path.[9] The ion beam is focused by a quadrupole magnet and is then analyzed by a 10° magnet. The analyzed ion beam passes through a differentially pumped gas-cell system into a 20° analyzing magnet for energy determination.

The differentially pumped gas-cell system is shown in Fig. 1. The gas cell is a 3-in.-o.d. $1\frac{3}{8}$-in.-i.d. stainless-steel cylinder 7.910 in. in length. Each end of the cell is sealed with four $\frac{3}{16}$-in.-thick brass disks tapered to 0.020-in. thickness near the axis, with each disk containing a 0.060-in.-diam aperture (except for H_2 when a 0.040-in.-diam aperture was used). The cell is mounted concentrically in a 6-in.-i.d. cylinder 11.81 in. in length, which constitutes the first differential-pumping section. The target gas leaks from the gas cell into the first differential-pumping section and is pumped away by a 1500-liter/sec 6-in. oil diffusion pump. Second differential-pumping sections (4-in.-i.d. tees) are connected to each end of the first differential-pumping section. The gas leaking into the second differential-pumping sections through four $\frac{1}{8}$-in.-diam apertures on each end of the first differential-pumping section is pumped away by two 750-liter/sec 4-in. oil diffusion pumps (one for each pumping section).

An 18-in.-long mercury thermometer, −1 to 51 °C and accurate to 0.1 °C, is placed in thermal contact with the wall of the gas cell for temperature measurements. The gas-cell pressure, which varies from 1.4 to 10 mm Hg throughout the experiment, is measured with a McLeod gauge (Bendix Vacuum Corporation, type GM-100A). The gas-cell exit-slit opening and 20°-magnet entrance-slit opening are usually 0.007 in. or less to minimize angular dispersion effects in the 20°-magnet energy determination. The beam current ($\simeq 10^{-10}$ to 10^{-8} A with no gas and $\simeq 10^{-13}$ to 10^{-11} A with gas) is measured in a Faraday cup at the 20° exit port with a Keithley Model 610C electrometer. An aperture of 0.010-in.-thick Ta, $\frac{1}{8}$-in. wide, and $\frac{1}{2}$-in. high, is located at the exit of the 20° magnet. Ta slits of opening 0.008 in. are placed immediately in front of the Faraday cup.

The incident energy scale E_i is calibrated against known nuclear reactions[10] and is found to be linear

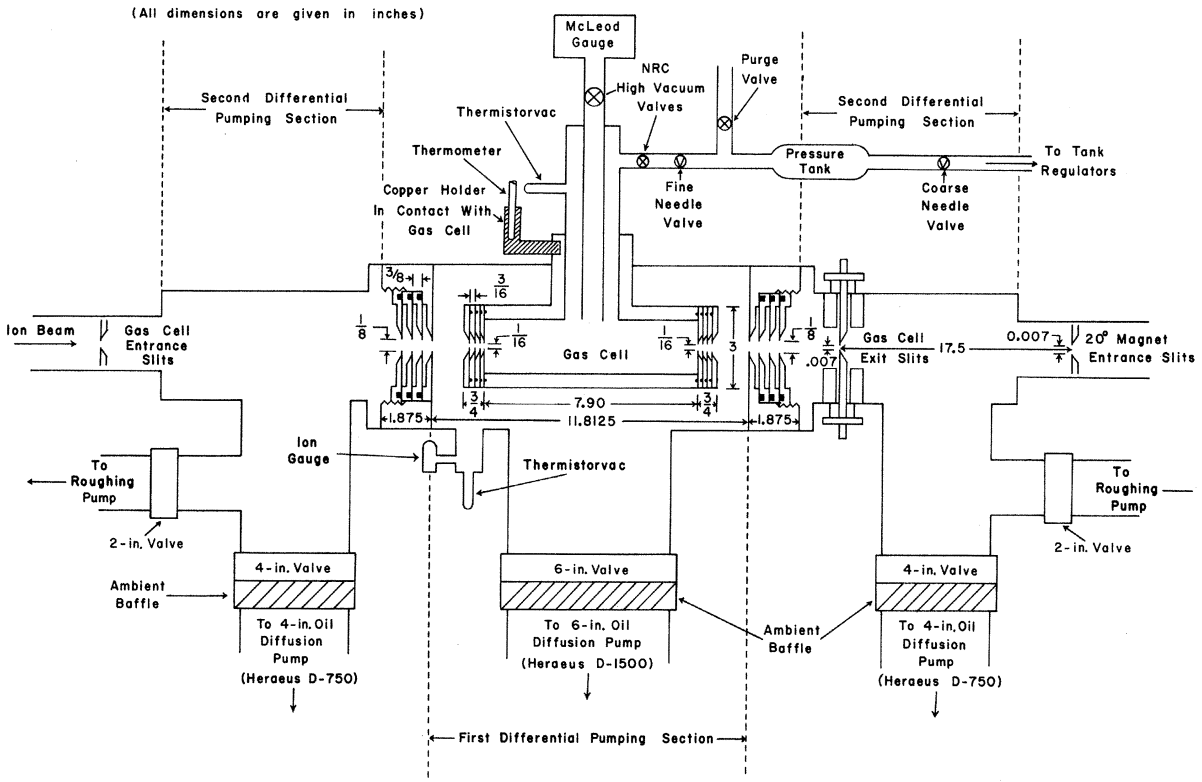

FIG. 1. Gas-cell system.

to better than 0.1%. For each energy-loss measurement the 20° magnet is calibrated against the incident energy scale, and the energy E_f after passing through gas in the cell is determined by the 20° magnet. The energy lost in passing through the cell was typically 100–200 keV and was within the limits $0.66 < E_f/E_i < 0.95$. The energy profile of the particles emerging from the gas cell within the small acceptance angle (0.0008 rad) of the 20° magnet is different from the energy profile of all particles emerging from the cell. This latter profile should be essentially symmetric as is verified by reference to Fig. 4 of Tschalär.[11] It is shown by Fastrup *et al.*[12] that the nuclear energy-loss distribution is still Gaussian for small acceptance angles, even though the tail of the distribution may be changed. The small acceptance angle into the magnet eliminates possible discrepancies between projected path and actual path. The energy profiles as measured at the Faraday cup at the indicated acceptance angles were symmetric throughout the course of the experiment. The symmetry of the peak was unaffected by using different pressures in the gas cell. All stopping cross-section measurements were run at different pressures to ensure that the results were independent of pressure. The energy E_f was determined from the maximum of the peak, and the most probable energy loss in the gas was taken to be $E_i - E_f$.

We have calculated the mean increase in energy loss $\overline{\delta T}_m$ due to multiple scattering by the method described by Tschalär and Bichsel.[13] The beam-intensity normalization factor N_α/N was obtained by integrating the angular distributions for multiple scattering from the approximate NSW theory as given by Marion and Zimmerman.[14] In our experiment, $\overline{\delta T}_m$ was of the order of 50 eV for $E_\alpha = 300$ keV with 100-keV energy loss. At $E_\alpha = 2$ MeV, $\overline{\delta T}_m$ is of the order of 1 eV. The calculations were made for a ~60-μg/cm^2 oxygen target. In all our measurements the mean increase in energy loss $\overline{\delta T}_m$ contributes no greater than a fraction of 0.1% at all energies and at all pressures used in the experiment. We have therefore neglected multiple-scattering energy corrections in the analysis of our data.

The stopping cross section ϵ of a gas in terms of the energy loss $E_i - E_f$, path length Δx, gas pressure P, and gas temperature T is

$$\epsilon = (E_i - E_f)/(N\Delta x), \quad N = 9.656\times10^{15}\,P/T\,, \qquad (1)$$

where ϵ is in 10^{-15} eV cm^2/molecule, E_i and E_f are in keV, P is in mm Hg, and T is in °K. The number N of molecules per cubic centimeter is obtained from the ideal-gas law. The length Δx is 21.505 cm, except when end corrections are needed be-

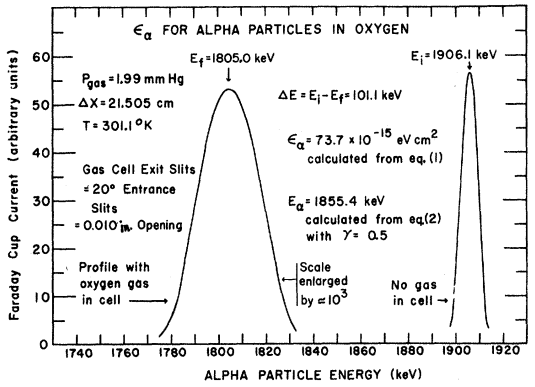

FIG. 2. Typical energy profile for the measurement of the stopping cross section of α particles in oxygen gas. The narrow peak at 1906.1 keV is with no gas in the cell, and the broad peak at 1805.0 keV is obtained with gas in the cell at pressure 1.99 mm Hg and T = 301.1 °K. The parameters used in Eqs. (1) and (2) to calculate ϵ_α at E_α are given.

cause of pressures in the first differential-pumping section being of the same order of magnitude as the pressure in the gas cell. A McLeod gauge containing triply distilled Hg was used to read the pressure in the first and second differential-pumping sections as a function of the gas-cell pressure. From these pressure relations and the physical length of the sections of the gas-cell system, the end corrections were calculated for each gas used in the experiment. The maximum end correction was 5% for H_2 and was no more than 2.5% for all other gases.

The energy E_α at which the stopping cross section is measured is given by Chilton, Cooper, and Harris[15] to be

$$E_\alpha = E_{av}\left[1+\frac{\gamma-1}{24}\left(\frac{\Delta E}{E_{av}}\right)^2+\cdots\right], \qquad (2)$$

where $E_{av}=\frac{1}{2}(E_i+E_f)$, $\Delta E=E_i-E_f$, and where γ is obtained from the relation $\epsilon=kE^{-\gamma}$. An iterative procedure was used by first obtaining a stopping cross-section curve as a function of E_{av}, then differentiating the lnϵ-vs-ln$E$ curve to find γ as a function of energy, and finally to use this γ to calculate E_α. The correction to E_{av} was less than 1.8 keV at 300 keV and less than 0.3 keV at 2 MeV. The corrections to ϵ were nowhere greater than 0.23%, but have been included.

A typical energy profile is given in Fig. 2 for the measurement of the stopping cross section of α particles in oxygen gas. The narrow peak centered at E_i = 1906.1 keV was obtained with no gas in the cell by varying the 20°-magnet current monotonically in narrow steps and reading the Faraday-cup current at each step with the Keithley meter (1-nA scale) while keeping the Van de Graaff energy fixed. Gas was then admitted into the cell and after the pressure had stabilized at 1.99 mm Hg, the Keithley current meter was switched to the pA scale, and the 20°-magnet current was again changed in discrete steps to obtain the indicated profile. Both curves, with and without gas, are symmetric in energy. For the profile given in Fig. 2, the gas-cell exit slits and the 20° entrance

TABLE I. Typical values of E_i, E_f, P, T, and Δx used in Eq. (1) to calculate $\epsilon_\alpha(O_2)$ as a function of energy E_α. E_α is determined from Eq. (2) with $\gamma=-0.3$ at 300 keV to +0.5 at 2 MeV. For pressures below 2.25 mm Hg, no end correction was needed on Δx. The end correction was as high as (21.84−21.50)×100%/21.50 = 1.58% for P = 5.12 mm Hg.

E_i (keV)	E_f (keV)	ΔE (keV)	E_α (keV)	P_{gas} (mm Hg)	Temp (°K)	Δx[a] (cm)	ϵ (10^{-15} eV cm^2)
374.4	280.2	94.2	325.8	1.62	302.8	21.50	84.8
374.4	294.4	80.0	333.4	1.39	302.8	21.50	83.9
697.5	443.4	254.1	565.7	3.82	302.7	21.76	95.8
697.4	489.8	207.6	590.6	3.12	302.7	21.61	96.5
697.3	566.5	130.8	630.9	1.96	302.7	21.50	97.3
1003.0	773.2	229.8	885.6	3.44	302.6	21.70	96.5
1002.6	722.2	280.4	858.6	4.14	302.6	21.80	97.4
1234.7	991.9	242.8	1111.3	3.78	302.2	21.77	92.3
1234.7	900.5	334.2	1064.3	5.12	302.2	21.84	93.5
1569.8	1346.9	222.9	1457.5	3.83	300.4	21.77	83.2
1570.1	1419.9	150.2	1494.6	2.62	300.4	21.53	82.8
1710.8	1507.2	203.6	1608.5	3.67	301.1	21.73	79.6
1710.8	1565.1	145.7	1637.8	2.65	301.1	21.53	79.6
1910.3	1773.6	136.7	1840.3	2.66	301.4	21.53	74.5
1910.3	1718.0	192.3	1913.6	3.69	301.4	21.74	74.8
2046.5	1851.3	195.2	1948.5	3.75	301.0	21.76	74.6
2136.5	1949.0	187.5	2042.4	3.75	301.0	21.76	71.6

[a] $\Delta x = (21.50 + 8.51\,P_1/P_{gas})$ cm, where 21.50 is the effective length of the gas cell. 8.51 is the effective length of the first differential-pumping system; P_{gas} = pressure in the gas cell; P_1 = pressure in the first differential-pumping system.

slits were fixed at a 0.010-in. opening. From the maximum of each peak, one can calculate $\Delta E = E_i - E_f$ to be 101.1 keV. This energy loss, along with $P_{gas} = 1.99$ mm Hg, $\Delta x = 21.505$ cm, and $T = 301.1$ °K, is inserted into Eq. (1) to obtain $\epsilon_\alpha = 73.7 \times 10^{-15}$ eV cm^2. The energy E_α at which ϵ_α is calculated is found from Eq. (2) to be 1855.4 keV.

Table I lists typical values of E_i, E_f, P, T, and Δx that were used for calculation of ϵ_α for O_2 as a function of E_α. The table is for oxygen, which is typical of the other 12 gases used in the experiment.

In Table I it is seen that for the three different pressures 1.96, 3.12, and 3.82 mm Hg used at $E_i = 697$ keV, the corresponding mean energy loss ΔE is 130.8, 207.6, and 254.1 keV, respectively. That is to say, when the pressure was essentially doubled, the mean energy loss also was doubled, but the same ϵ_α was obtained within experimental accuracy. For ϵ_α in N_2 at $T \simeq 301$ °K, an attempt was made to keep the average energy E_{av} approximately constant over a rather broad pressure range to see what effect the target thickness would have on the measurements. The pressures used were 1.47, 2.01, 2.81, 3.50, and 4.60 with corresponding mean energy loss $\Delta E = 96.8$, 132.7, 188.8, 235.0, and 312.1 keV and $\epsilon_\alpha = 95.5$, 95.7, 98.0, 95.5, and 95.5×10^{-15} eV cm^2, respectively. The average energy E_{av} varied from 883 to 831 keV for these measurements. A similar test was made in O_2 gas at 1.9 MeV using six pressures (2.07–5.01 mm Hg), with ΔE varying from 104 to 268 keV and $\epsilon_\alpha(O_2)$ varying from 72.8 to 75.8×10^{-15} eV cm^2.

The energies E_i and E_f, corresponding to the maximum of the peaks without gas and with gas, respectively, were usually obtained by visually searching for the maximum current I_{FC} at the Faraday cup without gas and with gas. This "peaking method" of searching for the maximum of the peak is meaningful only if the profiles such as in Fig. 2 are symmetric. The symmetry of the profiles was tested at $E_i \simeq 0.4$–0.5, $\simeq 1.0$, $\simeq 1.5$, and $\simeq 2.0$ MeV for the various gases. Approximately 1600 stopping cross-section measurements were made in the course of the experiment.

The measurements for α particles in N_2 were used as a reference standard throughout the course of the experiment. Periodically the N_2 measurements were rechecked to ensure that no drift or systematic error had been introduced at some stage in the experiment. The McLeod gauge was cleaned once during the course of the experiment by a professional glassblower, and the mercury used in the gauge was purified by triple distillation in a distilling apparatus. It is essential that at all times the mercury and the internal glassware of the gauge be clean so that the mercury does not rise erratically in the capillary and give erroneous readings. Toward the end of the experiment a second McLeod gauge, identical to the first, was purchased and the readings on the two gauges were compared. For all gases except H_2 the gas-cell pressures used were between $\simeq 1.4$ and 5 mm Hg (for H_2 the pressures, typically, were close to 10 mm Hg), and the readings on the two gauges agreed to better than 0.5% for all pressures greater than 1.4 mm Hg. The good agreement of the pressure readings from the two gauges coupled with the remeasurement of ϵ_α of N_2 as a reference standard periodically throughout the experiment gives strong support to the reliability of the measurements and to the elimination of any large systematic error from the McLeod gauge.

Independent measurements for H_2 and N_2 were also made in a sealed gas cell in an 18-in. scattering chamber, to test the reliability of the differentially pumped gas-cell measurements and to ensure that there was no large systematic error due to a dispersion effect in the energy determination with the 20° magnet. These independent measurements also ensure against any systematic error in the gas-cell measurements other than the energy calibration of the source and the pressure, since the same McLeod gauge was used with the sealed gas cell as was used with the differentially pumped gas cell. The separate measurements also ensure against any possible slit effects with the differentially pumped cell, against erroneous end corrections to the length of the gas cell, or against any possible heating effect from the primary α-particle beam, since a scattered α-particle beam penetrating the gas in the sealed gas cell would be greatly reduced in intensity. For these separate measurements, the α-particle beam was scattered from a Ta target and detected by a solid-state detector (at a laboratory angle of 130°), which determined the α-particle beam energy incident upon the sealed cell. The gas cell (length 9.55 cm) was sealed with 4×10^{-6}-in. Ni-foil windows obtained from Chromium Corporation of America, Waterbury, Conn. The cell was mounted on a rotating table in the scattering chamber so that the cell could be moved into and out of the scattered ion beam as desired. Three energies were determined: E_0, the energy of the ion scattered from the Ta; E_f, the ion energy with the Ni-foil windows only in the scattered ion beam; E_g, the ion energy with gas plus foils in the beam. The energy loss in gas was determined by a method similar to that of Reynolds *et al.*[6] but with the following modifications: (a) The energy profiles were a function of transmitted energy rather than incident energy, i.e., the incident energy was fixed, and (b) Ni-foil windows were used rather than Al-foil windows along with the dE/dx of Ni from Chu and Powers.[16] Pressure and temperature measurements were

made with the McLeod gauge and Hg thermometer, respectively, as in the differentially pumped system. The differentially pumped system was used in the majority of the measurements because of its greater intrinsic accuracy and greater speed in obtaining the data.

III. LOCALIZED HEATING EFFECTS

Some consideration must be given to local heating effects in the gas in the differentially pumped gas cell caused by the energy dissipation of the α-particle beam as it passes through the cell. For the small gas volume through which the beam actually passes, the following calculations apply: thickness (length) of small gas volume, $t = 50\ \mu g/cm^2$; area of beam, $A = 2\ mm^2 = 2\times10^{-2}\ cm^2$ ($\frac{1}{16}$-in. diam); total mass of gas traversed by beam, $m = At = 1\ \mu g$; power dissipated in gas at 10^{-9} A and $\Delta E = 100$ keV, $P = 10^{-4}\ W = 0.23\times10^{-4}$ cal/sec, which would cause a possible temperature increase per sec of $\Delta T = P/ms = 0.23\times10^{-4}/(10^{-6}\times0.22) = 100°/$sec. Since, according to Eq. (1), ϵ is proportional to T, the stopping cross-section measurement would be greatly in error if such a large temperature increase occurred. Since such a dramatic temperature increase was not observed at the Hg thermometer in thermal contact with the heavy gas-cell wall, one would either conclude that the temperature reading at the gas cell was not the one that should be used in Eq. (1), or that the heat from the small gas volume is rapidly transferred to its ambient surroundings, so that thermal equilibrium is achieved.

The separate gas-cell measurements in the scattering chamber provide a test of possible heating effects. If the heating effect there can be shown to be negligible, and if the same stopping cross-section measurement is obtained in the low-intensity scattered beam as is obtained in the higher-intensity primary beam, then one can conclude that localized heating effects do not introduce errors into our measurements.

For 2-MeV α particles scattered from Ta, we find

$$N_{out}/N_{inc} = N_{targ}\,\Delta x(d\sigma/d\Omega)\,d\Omega\ ,$$

where

$$N_{targ}\,\Delta x \simeq 0.66\times10^{19}\ cm^{-2},$$

$$\frac{d\sigma}{d\Omega} \simeq 10\times10^{-24}\ cm^2\ (\theta_{lab}\simeq 130°),$$

and

$$d\Omega \simeq 0.16\times10^{-4}\ sr.$$

This gives $N_{out}/N_{inc} \simeq 1.2\times10^{-9}$. For 300-keV α particles, $N\Delta x$ is decreased by a factor of $\simeq 10$, $d\sigma/d\Omega$ increases by $[(2\ MeV)/(0.3\ MeV)]^2 \simeq 40$, or N_{out}/N_{inc} increases by a factor of 4. Therefore at 2 MeV, for $N_{inc} \simeq 1\ \mu A$, $N_{out} \simeq 1.2\times10^{-6}$ nA and $N_{out} \simeq 4.8\times10^{-6}$ nA at 300 keV. The same identical stopping cross section was obtained for the gas (nitrogen and hydrogen) in the scattered beam in the scattering chamber as was obtained for these gases in the differentially pumped gas cell in the primary α-particle beam. That is to say, even if the temperature should rise by 100 deg/sec in the direct

TABLE II. Experimental precision of the α-particle stopping cross-section measurements in gases using the differentially pumped gas-cell system.

Source of error	Probable error in source	Probably error in ϵ_α from this source
E_i Uncertainty in incident energy E_i due to		
(i) Statistical fluctuation due to instability of corona stabilizer system	$<\pm0.5$ keV	$<\pm0.5\%$
(ii) Uncertainty determined from maximum of the peak in incident energy profile	±0.5 keV	$\pm0.5\%$
E_f Uncertainty in final energy E_f after passing through gas-cell system as determined from maximum of the peak in the final energy profile	±1.0–2.0 keV	1.0–2.0%
T Uncertainty in gas temperature	±0.1 °K	$\pm0.03\%$
P Uncertainty in gas pressure due to		
(i) Lack of stabilization of pressure in gas cell after pressure is changed or gas is admitted into gas cell	$\pm0.7\%$	$\pm0.7\%$
(ii) Parallax and reading errors of McLeod gauge	±0.005 mm Hg	$\pm0.5\%$
	rms probable error:	1.5–2.3%

TABLE III. Gas Purity.

Gas	Minimum purity (%)	Principal impurity
H_2	99.95	N_2
N_2	99.995	O_2
O_2	99.5	Ar
N_2O	98.0	Air
NH_3	99.9	H_2O
CO	99.5	CO_2
CO_2	99.99	N_2
CH_4	99.95	N_2
C_2H_2	99.6	Air
C_2H_4	99.5	CH_4
C_2H_6	99.0	C_2H_4
C_3H_6 (propylene)	99.0	C_3H_8
$(CH_2)_3$ (cyclopropane)	99.0	Air

beam, it would rise by $\frac{1}{2}\times 4.8\times 10^{-6}\times 100$ deg/sec (the factor of $\frac{1}{2}$ comes from the fact that the separate gas cell was only 9.55 cm in length, i.e., $\simeq\frac{1}{2}$ the length of the first one) $= 2.4\times 10^{-4}$ deg/sec $= 0.9$ deg/h in the separate sealed gas-cell measurement at 300 keV ($\simeq 0.22$ deg/h at 2 MeV). The measurement in the scattering chamber took, typically, about 20 min per point, which corresponds to 0.3 deg/half-hour (0.3 deg compared to 300 °K the typical gas-cell temperature), i.e., only a 0.1% effect on the stopping cross-section measurement at 300 keV and a 0.02% effect at 2 MeV. Since the same stopping cross sections were observed in the two separate gas-cell systems, one can only conclude that the heat rise in the direct beam must be quickly transferred to its ambient surroundings which act as a heat sink, and that our separate measurements in N_2 (N_2 was used as our reference standard in all the measurements) at a considerably reduced beam intensity confirm that our experimental technique using a direct beam in the differentially pumped system is quite all right insofar as localized heating effects are concerned.

IV. ERRORS

In Table II the source of error is listed along with the estimated probable error in this source, and the probable error in the stopping cross-section measurement ϵ_α from this source. The largest source of error lies in the difficulty of locating precisely the maximum of the peak E_f in the energy profile with gas in the cell. The next-to-largest source results from not allowing the gas pressure to stabilize in the gas cell after the gas has been admitted into the cell or after the pressure is changed. Typically, the gas was pumped out of the cell, the pressure was read to ensure that there was no residual gas in the cell, and then the gas was admitted to the cell. Normally 5–10 min elapsed in waiting for the pressure to stabilize in

TABLE IV. Energy loss of α particles in various gaseous compounds. Column 1 gives the stopping material. Column 2 gives the α-particle energy; column 3, the stopping cross section ϵ_α; column 4, the energy loss; and column 5, the probable error.

Gas	Energy (keV)	ϵ_α (10^{-15} eV cm^2)	$dE/\rho\,dx$ (keV cm^2/μg)	Probable error (%)
CH_4	300	88.2	3.31	1.0
	400	97.1	3.64	1.0
	500	102.0	3.83	1.0
	600	103.2	3.88	1.0
	700	102.0	3.83	1.0
	800	99.0	3.72	1.0
	900	95.5	3.59	1.1
	1000	91.7	3.44	1.1
	1100	87.4	3.28	1.2
	1200	83.2	3.12	1.2
	1300	79.7	2.99	1.2
	1400	76.0	2.85	1.2
	1500	72.9	2.74	1.2
	1600	70.0	2.63	1.2
	1700	66.8	2.51	1.2
	1800	64.4	2.42	1.5
	1900	62.3	2.34	1.5
	2000	60.5	2.27	1.5
C_2H_2	300	109.2	2.52	1.0
	400	117.6	2.72	1.0
	500	124.2	2.87	1.0
	600	125.7	2.91	1.5
	700	122.9	2.84	1.5
	800	119.6	2.77	1.5
	900	115.2	2.67	1.5
	1000	110.8	2.56	1.5
	1100	106.5	2.46	1.2
	1200	102.2	2.36	1.2
	1300	98.0	2.27	1.2
	1400	94.4	2.18	1.2
	1500	90.4	2.09	1.2
	1600	87.2	2.02	1.5
	1700	84.2	1.95	1.5
	1800	81.3	1.88	1.5
	1900	78.4	1.81	1.5
	2000	76.0	1.76	1.5
C_2H_4	300	125.0	2.70	1.3
	400	137.9	2.96	1.3
	500	145.2	3.12	1.3
	600	147.4	3.17	1.3
	700	145.5	3.13	1.3
	800	142.2	3.06	1.3
	900	137.0	2.94	1.3
	1000	132.0	2.84	1.3
	1100	127.3	2.74	1.3
	1200	122.3	2.63	1.1
	1300	116.9	2.51	1.1
	1400	111.6	2.40	1.1
	1500	106.7	2.29	1.1
	1600	102.8	2.21	2.0
	1700	99.2	2.13	2.0
	1800	95.8	2.06	2.0
	1900	93.0	2.00	2.0
	2000	90.0	1.93	2.0

TABLE IV. (*Continued*)

Gas	Energy (keV)	ϵ_α (10^{-15} eV cm^2)	$dE/\rho\,dx$ (keV cm^2/μg)	Probable error (%)
C_2H_6	300	147.2	2.94	2.0
	400	161.8	3.24	1.0
	500	170.0	3.41	1.0
	600	173.7	3.48	1.0
	700	171.5	3.44	1.0
	800	166.7	3.34	1.0
	900	160.8	3.22	1.0
	1000	155.0	3.11	1.0
	1100	149.2	2.99	1.0
	1200	142.7	2.86	1.0
	1300	136.5	2.73	1.0
	1400	130.0	2.60	1.0
	1500	124.4	2.49	1.5
	1600	119.7	2.40	1.5
	1700	115.2	2.31	1.5
	1800	111.0	2.22	1.5
	1900	107.2	2.15	1.5
	2000	104.0	2.08	1.5
C_3H_6	300	179.9	2.58	1.2
	400	202.3	2.89	1.0
	500	213.1	3.05	1.0
	600	216.2	3.09	1.0
	700	215.3	3.08	1.0
	800	209.7	3.00	1.0
	900	203.7	2.92	1.0
	1000	196.2	2.81	1.0
	1100	188.7	2.70	1.0
	1200	181.4	2.60	1.5
	1300	173.8	2.49	1.5
	1400	165.8	2.37	1.5
	1500	158.2	2.26	1.5
	1600	151.1	2.16	1.8
	1700	144.7	2.07	1.8
	1800	139.1	1.99	1.8
	1900	134.3	1.92	1.8
	2000	130.4	1.87	1.8
$(CH_2)_3$	300	179.9	2.58	1.0
	400	203.1	2.90	1.0
	500	215.1	3.08	1.2
	600	217.5	3.11	1.2
	700	216.5	3.10	1.2
	800	210.7	3.02	1.2
	900	204.3	2.92	1.0
	1000	196.0	2.81	1.0
	1100	187.8	2.69	1.0
	1200	180.2	2.58	1.0
	1300	173.0	2.48	1.0
	1400	165.2	2.36	1.0
	1500	159.0	2.28	1.5
	1600	152.2	2.18	1.5
	1700	145.8	2.09	1.5
	1800	140.1	2.01	1.5
	1900	135.5	1.94	1.5
	2000	131.4	1.88	1.5

TABLE IV. (*Continued*)

Gas	Energy (keV)	ϵ_α (10^{-15} eV cm^2)	$dE/\rho\,dx$ (keV cm^2/μg)	Probable error (%)
H_2	300	26.6	7.95	1.5
	400	28.0	8.37	1.5
	500	29.0	8.66	1.5
	600	28.8	8.60	1.5
	700	28.0	8.37	1.5
	800	27.0	8.07	1.5
	900	25.9	7.74	1.5
	1000	24.8	7.41	1.5
	1100	23.6	7.05	1.5
	1200	22.4	6.69	1.5
	1300	21.3	6.36	1.5
	1400	20.2	6.04	1.5
	1500	19.2	5.73	1.5
	1600	18.3	5.47	1.5
	1700	17.4	5.20	1.5
	1800	16.7	4.99	1.5
	1900	16.0	4.78	1.5
	2000	15.5	4.63	1.5
N_2	300	86.1	1.85	1.5
	400	93.3	2.00	1.5
	500	96.7	2.08	1.5
	600	97.7	2.10	1.5
	700	97.3	2.09	1.5
	800	96.2	2.07	1.5
	900	94.4	2.03	1.5
	1000	92.1	1.98	1.5
	1100	89.4	1.92	1.5
	1200	86.6	1.86	1.5
	1300	83.6	1.80	1.5
	1400	80.8	1.74	1.5
	1500	78.0	1.68	1.5
	1600	75.3	1.62	2.0
	1700	72.9	1.57	2.0
	1800	70.7	1.52	2.0
	1900	68.5	1.47	2.0
	2000	66.4	1.43	2.0
O_2	300	81.8	1.54	1.0
	400	89.0	1.67	1.0
	500	93.4	1.76	1.0
	600	96.0	1.81	1.0
	700	97.0	1.83	1.0
	800	96.9	1.82	1.0
	900	96.0	1.81	1.0
	1000	94.4	1.78	1.0
	1100	92.4	1.74	1.0
	1200	90.2	1.70	1.5
	1300	87.8	1.65	1.5
	1400	85.3	1.61	1.5
	1500	82.8	1.56	1.5
	1600	80.4	1.51	2.0
	1700	78.2	1.47	2.0
	1800	76.2	1.43	2.0
	1900	74.0	1.39	2.0
	2000	72.0	1.36	2.0

the cell. After ϵ_α had been measured at this pressure, the pressure was then increased (or decreased) to another reading, and a new ϵ_α was determined. Two or three different pressures were used for each E_i. The rms probable error is given by the square root of the sums of the squares of these

TABLE IV. (*Continued*)

Gas	Energy (keV)	ϵ_α (10^{-15} eV cm^2)	$dE/\rho\,dx$ (keV cm^2/μg)	Probable error (%)
NH_3	300	76.8	2.72	1.0
	400	82.8	2.93	1.0
	500	87.0	3.08	1.0
	600	88.8	3.14	1.0
	700	88.5	3.13	1.2
	800	86.4	3.06	1.2
	900	83.5	2.95	1.2
	1000	80.5	2.85	1.2
	1100	77.8	2.75	1.2
	1200	74.8	2.65	1.2
	1300	72.3	2.56	1.2
	1400	69.6	2.46	1.2
	1500	67.0	2.37	1.5
	1600	64.7	2.29	1.5
	1700	62.4	2.21	1.5
	1800	60.3	2.13	1.5
	1900	58.0	2.05	1.5
	2000	56.0	1.98	1.5
N_2O	300	120.6	1.65	1.1
	400	134.2	1.84	1.1
	500	140.1	1.92	1.4
	600	142.6	1.95	1.4
	700	142.9	1.96	1.4
	800	142.7	1.95	1.4
	900	141.9	1.94	1.4
	1000	139.4	1.91	1.4
	1100	134.7	1.84	1.4
	1200	129.9	1.78	1.2
	1300	125.1	1.71	1.2
	1400	120.6	1.65	1.2
	1500	116.7	1.60	1.2
	1600	112.9	1.55	1.5
	1700	109.3	1.50	1.5
	1800	105.5	1.44	1.5
	1900	102.6	1.40	1.5
	2000	99.9	1.37	1.5
CO	300	84.6	1.82	1.0
	400	91.2	1.96	1.0
	500	94.8	2.04	1.0
	600	95.5	2.05	1.0
	700	95.3	2.05	1.0
	800	94.2	2.03	1.0
	900	92.5	1.99	1.0
	1000	90.3	1.94	1.0
	1100	87.8	1.89	1.2
	1200	85.1	1.83	1.2
	1300	82.4	1.77	1.2
	1400	79.8	1.72	1.2
	1500	77.2	1.66	1.2
	1600	74.8	1.61	1.5
	1700	72.5	1.56	1.5
	1800	70.5	1.52	1.5
	1900	68.7	1.48	1.5
	2000	67.2	1.45	1.5

errors.

The gases were obtained from Matheson Company, La Porte, Tex. The minimum purity and

TABLE IV. (*Continued*)

Gas	Energy (keV)	ϵ_α (10^{-15} eV cm^2)	$dE/\rho\,dx$ (keV cm^2/μg)	Probable error (%)
CO_2	300	118.2	1.62	1.0
	400	130.3	1.78	1.0
	500	137.0	1.88	1.0
	600	140.7	1.93	1.0
	700	141.7	1.94	1.0
	800	140.7	1.93	1.0
	900	138.8	1.90	1.0
	1000	136.2	1.87	1.0
	1100	133.1	1.82	1.0
	1200	129.6	1.77	1.0
	1300	125.8	1.72	1.0
	1400	122.1	1.67	1.0
	1500	118.4	1.62	1.0
	1600	114.9	1.57	1.0
	1700	111.6	1.53	1.0
	1800	108.6	1.49	1.0
	1900	106.0	1.45	1.5
	2000	103.2	1.41	1.5

principal impurity of each gas as given by the supplier are given in Table III. Since N_2O has the least purity (98.0%), a correction was made to the measured $\epsilon(N_2O)$ based on 98.0% N_2O, 2% air (80% N_2, 20% O_2). The corrected values of $\epsilon(N_2O)$ are the ones tabulated in Table IV, and differ by no more than 0.7% from the uncorrected values. The maximum effect upon the measurements due to gas impurities is $< 0.2\%$.

Since all the gases were admitted into the cell through the same fine metering valves, it is possible that some contamination occurred due to residual gas being left in the pressure tank (see Fig. 1). Before a new gas was used, the pressure tank was carefully pumped out by opening the metering valves until the McLeod gauge read less than 0.001 mm Hg. The NRC valve to the supply bottle was then closed, and the new gas was purged several times through the purge value before ϵ_α measurements were made with the new gas. The repeated consistency of the N_2 measurements, used as a standard and made throughout the course of the experiment, minimizes the possibility of gas contamination being a source of error.

The maximum total error of the sealed gas-cell data was calculated in a manner similar to that of Reynolds *et al.*, as modified by the errors associated with the solid-state detector electronics as given by Chu and Powers, and was found to be 3.4% for the H_2 and N_2 data.

The random errors listed in Table II represent the error of a single measurement. An average of 122 data points was obtained for each gas measured, and these points determined an average-value curve, which was drawn through the points.

This curve gives an ϵ_α (average) at each energy. From the quantity

$$\sigma^2 = \{\sum_k [\epsilon_\alpha(\text{av}) - \epsilon_\alpha{}^{(k)}]^2\}/(n-1) ,$$

calculated for each curve, it was anticipated that 68% of the points would be within $\pm\sigma$ of the curve, 96% within $\pm 2\sigma$ of the curve, etc. What was found, however, was that for a given energy region, say, 1.2–1.5 MeV, more than 68% of the points were within $\pm\sigma$ of the curve, and in another region, say, 1.6–2.0 MeV, less than 68% of the points were within $\pm\sigma$. The total energy region 0.3–2.0 MeV was therefore divided into subregions, a σ was calculated for each subregion and was checked to ensure that 68% of the points were within $\pm\sigma$, 96% within $\pm 2\sigma$, etc., and this σ was taken to be the standard deviation. The σ's were multiplied by 0.6745 and were entered into Table IV as probable errors. These probable errors vary from 1.0 to 2.0% and are seen to be in reasonable agreement with the probable-error assignment of a single measurement given in Table II.

V. RESULTS

The stopping cross sections are given in Table IV at 100-keV intervals as read from the average-value curve along with $dE/\rho dx$ and total probable error. In Fig. 3 a typical stopping cross-section curve is shown. The individual measurements are plotted as ×'s, the average-value curve as a solid line, and the measurements by Rotondi[3] as solid triangles.

The sealed gas-cell measurements agree with the differentially pumped gas-cell measurements to within ±2.1% for H_2 and ±2.7% for N_2. The independent measurements by Palmer[2] and Rotondi[3] agree with the present measurements to within 0 to 21%. At 2 MeV eight out of ten of their measurements agree to the present measurements to within 2.3%; at 1.5 MeV seven of their measurements agree with the present measurements to within 3.2%; at 1.0 MeV five out of ten of their measurements agree with the present ones within 5.1%; at 0.5 MeV two out of the four measurements agree with the present ones within 3.5%. The 1.0-MeV point in H_2 is 21% lower than the value obtained in the present experiment; however, the 2-MeV point agrees to within 1.3%. The generally good agreement of these independent measurements with those of the present experiment gives strong support to the reliability of the present data and also gives evidence that there is no large systematic error in the present experiment.

The analysis[8] of the data indicated that the acetylene stopping cross-section measurement deviated from Bragg's rule; the source of the deviation was attributed to either a chemical-binding effect or to a possible impurity in the C_2H_2. The manufacturer

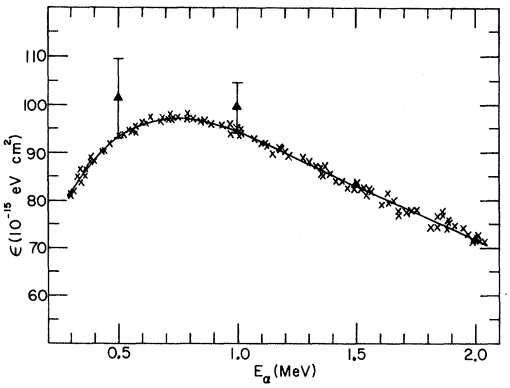

FIG. 3. Stopping cross section of oxygen gas for α particles as a function of the α-particle energy. ×'s are the present measurements, the smooth curve is an average-value curve drawn through these measurements, and the triangles are measurements by Rotondi (Ref. 3).

(Matheson Co., La Porte, Tex.) indicated that contamination of the sample by acetone was possible since the acetylene was shipped dissolved in acetone in which it is highly soluble at pressures of 175 lb/in.^{2} or greater. A new cylinder of acetylene was obtained, an entire new set of measurements were made, and the stopping cross sections were identical to those obtained previously. A gas-chromatograph test was run on the sample, and the acetone content was only (8×10^{-4})% of the total volume of the sample. The test showed that the purity as listed in Table I by the manufacturer was quite reasonable, and that the deviation from Bragg's rule for acetylene was therefore substantiated.

It is also shown in the analysis[8] that the carbon stopping cross sections calculated from gaseous media deviate from the measured values of Chu and Powers[16] in solid carbon thin films by as much as 22.4% at 400 keV to 13% at 2 MeV. The independent measurements by Porat and Ramavataram[17] of α particles in carbon are higher by 15% at 400 keV, agree at 880 keV, and are lower by 6% at 1.3 MeV than those of Chu and Powers. Booth and Grant[18] found a discrepancy between their dE/dx measurements of O in C and the measurements of O in C by Porat and Ramavataram. They suggested that the differences in various measurements in evaporated C thin films may be due to the high tendency of carbon foils to adsorb water vapor, which may result in different stopping cross sections for foils prepared differently (see also Kalish *et al.*[19]) Although Booth and Grant, and Kalish *et al.* suggested this adsorption as a possibility, they did not measure the water-vapor adsorption on their carbon films to check the validity of their hypothesis.

The elastic scattering of α particles provides an excellent tool for checking surface contamination[20] if the impurities have higher atomic numbers

than the target backing. The measurements of dE/dx in C by Chu and Powers were done with a Ta backing for the C film which would not have been amenable to Rubin's technique for checking surface impurities. We therefore prepared a carbon thin film by evaporation onto a $\frac{1}{16}$-in.-thick polished Be plate. The procedure was identical to that used by Chu and Powers: using a carbon arc in a bell jar, admitting dry nitrogen gas to let the bell jar reach atmospheric pressure, weighing the sample with a microbalance, and then putting the sample in a scattering chamber. A vacuum as low as 10^{-5} mm Hg could be obtained in the scattering chamber within 5 to 10 min, and α particles were immediately scattered from the C on Be, and a spectrum on a multichannel analyzer was obtained. The time required to obtain the spectrum from the instant the sample was placed in the scattering chamber was no more than 12 min. The only contaminants found were small traces of nitrogen and oxygen. Two small oxygen peaks were found: one on the surface of the Be and one on the surface of the C. The N was also on the surface of the C. The areas under the large C "trapezoidal" peak and under the small N and O peaks on the surface of C were measured from the spectrum. If one assumes that the oxygen on the C surface was actually due to adsorbed water vapor, and that the elastic scattering was Rutherford, then the maximum error in the weight of the deposited C would be 3.8%. It was found by scattering α particles from the same target after delays of 8, 16, and 24 h that the small O and N surface peaks on the C disappeared, thus indicating that these adsorbed materials were being pumped out by the vacuum pumps. The elastic scattering was done at three different energies and on three separate C targets, each of different thickness, and essentially the same results were found each time. It was therefore concluded that the discrepancy between our measurements and those of Porat and Ramavataram was not due to water-vapor adsorption onto our thin films. It should be mentioned, however, that our films had only one surface exposed to air, whereas those used in a transmission experiment would have two surfaces exposed to air. For the latter films, the water-vapor adsorption would be doubled.

As a final check on the solid C dE/dx measurements, we used a different backing material than Ta. The Ta backing was only 0.005-in. thick, and it is possible that localized heating effects could cause peeling or possibly stretching of the C on the Ta. We used $\frac{1}{16}$-in.-thick polished Ni and Sn plates for backing materials. New measurements over the entire energy region of dE/dx in C were made on these backings with two different C thicknesses. The new measurements agreed completely with the original ones, and we therefore conclude that it is meaningful to use the original C dE/dx measurements in solids in the analysis to check the validity of Bragg's rule.

The analysis of the present data based on a study of the chemical binding of atoms in molecules is given in a separate paper.[8] It is shown there that Bragg's rule applies to 9 of the 13 gaseous compounds over the entire energy region 300 keV to 2 MeV; deviations from Bragg's rule as high as 12.8% occur for the compound C_2H_2. Also, the atomic stopping cross sections of H and O are given by one-half the measured molecular stopping cross sections, but this result does not apply to nitrogen. In addition, the atomic stopping cross section of carbon calculated from the stopping cross sections of gaseous compounds is shown not to be the same as carbon stopping cross sections obtained from solid thin films of carbon.

ACKNOWLEDGMENT

The authors wish to express their gratitude to Professor Ward Whaling for reading the manuscript prior to publication.

*Research supported in part by the Robert Welch Foundation, Houston, Tex.

[1]J. T. Park, Phys. Rev. 138, A1317 (1965).
[2]R. B. J. Palmer, Proc. Phys. Soc. (London) 87, 681 (1966).
[3]E. Rotondi, Radiation Res. 33, 1 (1968).
[4]E. Rotondi, National Research Council of Canada Report No. NRC-9076, 1966 (unpublished).
[5]W. H. Bragg and R. Kleeman, Phil. Mag. 10, S318 (1905).
[6]H. K. Reynolds, D. N. F. Dunbar, W. A. Wenzel, and W. Whaling, Phys. Rev. 92, 742 (1953).
[7]J. T. Park and E. J. Zimmerman, Phys. Rev. 131, 1611 (1953).
[8]P. D. Bourland and D. Powers, following paper, Phys. Rev. B 3, 3635 (1971).
[9]R. B. Brown, P. D. Bourland, and D. Powers, Nucl. Instr. Methods 72, 217 (1969).
[10]J. B. Marion, Rev. Mod. Phys. 38, 660 (1966).
[11]C. Tschalär, Nucl. Instr. Methods 61, 141 (1968).
[12]B. Fastrup, P. Hvelplund, and C. A. Sautter, Kgl. Danske Videnskab. Selskab, Mat.-Fys. Medd. 35, No. 10 (1966).
[13]C. Tschalär and H. Bichsel, Nucl. Instr. Methods 62, 208 (1968).
[14]J. B. Marion and B. A. Zimmerman, Nucl. Instr. Methods 51, 93 (1967).
[15]A. B. Chilton, J. N. Cooper, and J. C. Harris, Phys. Rev. 93, 413 (1954).
[16]W. K. Chu and D. Powers, Phys. Rev. 187, 478 (1969).
[17]D. I. Porat and K. Ramavataram, Proc. Phys. Soc. (London) 78, 1135 (1961).
[18]W. Booth and I. S. Grant, Nucl. Phys. 63, 481

(1965).
[19]R. Kalish, L. Grodzins, F. Chmara, and P. H. Rose, Phys. Rev. 183, 431 (1969).
[20]S. Rubin, Nucl. Instr. Methods 5, 177 (1959).

PHYSICAL REVIEW B VOLUME 3, NUMBER 11 1 JUNE 1971

Bragg-Rule Applicability to Stopping Cross Sections of Gases for α Particles of Energy 0.3–2.0 MeV*

P. D. Bourland and D. Powers
Baylor University, Waco, Texas 76703
(Received 22 July 1970)

The additivity of atomic stopping cross sections, Bragg's rule, is tested for α particles in the gaseous compounds H_2, N_2, O_2, NH_3, N_2O, CO, CO_2, CH_4, C_2H_2, C_2H_4, C_2H_6, C_3H_6 (propylene), and $(CH_2)_3$ (cyclopropane). Compounds with single and double bonds are found to obey Bragg's rule. Compounds containing triple-bond structure are found to deviate from Bragg's rule by as much as 12.8%, but an empirical triple-bond correction is made to fit all the data of the present experiment. Evidence is seen for a possible physical-state effect.

I. INTRODUCTION

The additivity of atomic stopping cross sections, Bragg's rule, was first stated by Bragg and Kleeman[1] in 1905. The stopping power of H_2O (in gas, liquid, and solid state) for α particles has been measured by many groups.[2–9] The results obtained by these groups are conflicting, and a consistent statement on Bragg's rule cannot be made from these measurements. The energy loss of α particles in gases has been measured by four groups.[10–14] Schmieder[10] noticed deviation from Bragg's rule for nitrogen-oxygen compounds, but not for carbon-oxygen or carbon-hydrogen compounds. Park[11] found no deviation from Bragg's rule for hydrocarbons. The measurements by Palmer[12] and by Rotondi,[13] using α particles of energy 1 MeV or above, also showed no deviation from Bragg's rule. The measurements by Reynolds *et al.*[15] and by Park and Zimmerman[16] for protons in gases, however, indicated a deviation from Bragg's rule below 150 keV. Thus, it might then be expected that deviations would occur for α-particle energies below 600 keV.

The experimental tests of Bragg's rule mentioned above may be classified broadly into two general categories: (a) physical-state effects (gas, liquid, or solid) and (b) chemical-binding effects. The purpose of the present experiment is to attempt to clarify some of the conflicting results of the above-mentioned experiments by concentrating on chemical-binding effects for gaseous compounds. The goal is to answer two questions: (a) Is Bragg's rule valid for a given class of compounds and a given energy region? (b) If Bragg's rule does not hold, what is the reason for it not holding, and can a correction be made to account for the deviation? Previous experiments have yielded answers to (a), but none have yielded the answer to (b) explicitly.

The experimental procedure, accuracy, results, and comparison with other measurements for α-particle stopping cross sections in H_2, N_2, O_2, CO_2, NH_3, N_2O, CO, CH_4, C_2H_2, C_2H_4, C_2H_6, C_3H_6, and $(CH_2)_3$ for 0.3–2-MeV α particles are given in a separate paper,[17] which will be referred to as I.

II. ANALYSIS OF DATA

A. Physical State and Chemical Binding

Bragg's rule may be stated as follows:

$$\epsilon(X_mY_n) = m\epsilon(X) + n\epsilon(Y), \tag{1}$$

where $\epsilon(X_mY_n)$ is the stopping cross section $dE/(Ndx)$ of the molecule X_mY_n, N is the number of molecules per unit volume, $\epsilon(X)$ and $\epsilon(Y)$ are the stopping cross sections of the atomic constituents X and Y, respectively. Deviations from (1) may be caused by physical-state effects, as for example, in the molecule CO_2 (a gaseous compound); ϵ(C) would usually be obtained from matter in the solid state and ϵ(O) from matter in the gaseous state. If the atomic substance is in a physical state different from that of the molecular substance of which it is a constituent, departures from the simple additivity rule may occur, since nothing regarding the physical state is considered in (1). Indeed, physical-state effects have been seen in molecular stopping data, such as the stopping power of H_2O vapor by Reynolds *et al.*[15] being an average of 11% higher than that of D_2O ice by Wenzel and Whaling[18] for protons of 30–600-keV energy. Palmer[9] found the stopping power to be higher in the vapor state than in the liquid state for low-energy α particles in water, ethyl alcohol, and carbon tetrachloride.